

Application of Partial Differential Equations in Multi Focused Image Fusion

K. Kannan

Department of Mechatronics Engineering, KAMARAJ College of Engineering and Technology, Madurai – 625 701
Email : kannan_kcet@yahoo.co.in

-----ABSTRACT-----

Image Fusion is a process used to combine two or more images to form more informative image. More often, machine vision cameras are affected by limited depth of field and capture the clear view of the objects which are in focus. Other objects in the scene will be blurred. So, it is necessary to combine set of images to have the clear view of all objects in the scene. This is called Multi focused image fusion. This paper compares and presents the performance of second order and fourth order partial differential equation in multi focused image fusion.

Keywords - Depth of field, Image Fusion, Multi focused image Fusion, Partial Differential Equations.

Date of Submission: Jun 21, 2022

Date of Acceptance: Jul 27, 2022

I. INTRODUCTION

Visual information in the scene is captured by CCD or CMOS cameras for machine vision applications. Due to limited Depth of Field (DOF) in machine vision cameras, it is possible to capture the clear image of the objects which are in focus only and other objects in the scene will be blurred [1]. In this situation, Multi focus image fusion is used to combines images of the same scene with different focus to form the composite image in which all objects are in clear focus. Many methods of multi focus image fusion are reported in literature. Among them, multi scale decomposition methods produce good results. But, these methods introduce artifacts in the fused image. To avoid these artifacts, fusion methods based on optimization were proposed. Optimization methods take multiple iterations to generate composite image and remove edge details. To preserve edge details in the final fused image, edge preserving fusion methods were introduced. Popular filters used in these methods are guided filter, bilateral filter, cross bilateral filter, anisotropic diffusion filter. These methods decompose each source image into approximation image and detail image. Fused images are formed by combining manipulated approximation image and detail image. Bilateral filter and cross bilateral filter fusion methods produces gradient reversal artifacts in the fused image whereas guided image fusion method produces halo effects in the fused image [2]. The use of second order Partial Differential Equations (PDE) in image denoising produces excellent results interns of edge preservation, but introduces staircase effect. To remove this stair case effect, non linear fourth order PDE are used. This paper compares and presents the performance of second order and fourth order PDE in multi focused image fusion. The following section overviews second order and fourth order PDEs proposed by Perona & Malik [3] and You & Kaveh [4] respectively. Section 3 presents the multi focused fusion methodology and Section 4 discuss the performance of second order and fourth order PDE. Finally, summary of this paper with conclusion is presented.

II. OVERVIEW OF PARTIAL DIFFERENTIAL EQUATIONS

The second order PDE smoothes a given image at coarser regions while preserving the edges. It uses intra-region smoothing to generate coarser images. At each coarser resolution, edges are sharp and meaningful. The second order PDE use the following flux function to control the diffusion of an image I as

$$I_{i,j}^t = c(x,y,t)\Delta I + \nabla_c \cdot \nabla I \quad \dots\dots (1)$$

where $c(x,y,t)$ = Flux function, Δ = Laplacian operator, ∇ = Gradient operator, t = Time or iteration [3]. The solution for this PDE is

$$I_{i,j}^{t+1} = I_{i,j}^t + \lambda [c_N \cdot \bar{\nabla}_N I_{i,j}^t + c_S \cdot \bar{\nabla}_S I_{i,j}^t + c_E \cdot \bar{\nabla}_E I_{i,j}^t + c_W \cdot \bar{\nabla}_W I_{i,j}^t \dots\dots (2)$$

In the above equation, $I_{i,j}^{t+1}$ is the coarser resolution image at $t + 1$ scale which depends on the previous coarser image $I_{i,j}^t$. λ is a stability constant which lies in the range $0 \leq \lambda \leq 1/4$. $\bar{\nabla}_N, \bar{\nabla}_S, \bar{\nabla}_E$ and $\bar{\nabla}_W$ & c_N, c_S, c_E and c_S are the nearest- neighbour differences & in flux functions north, south, east and west directions respectively. The model of fourth order PDE is given by

$$\frac{\partial I}{\partial x} = -\nabla^2 [c(|\nabla^2 I|)\nabla^2 I] \quad \dots\dots (3)$$

where is the $\nabla^2 I$ Laplacian of the image I [4]. Since the Laplacian of an image at a pixel is zero if the image is planar in its neighbourhood, the fourth order PDE attempt to remove noise and preserve edges. The diffusion functions $c(\cdot)$ are taken from Perona–Malik diffusivity functions. They are given by, $c(s) = 1 / [1 + (s/k)^2]$ and $c(s) = \exp[-(s/k)^2]$ and offer trade-off between the smoothing and edge preservation. First function is useful if the image consists of wide regions over the smaller regions. Second function is useful if the image consists of high-contrast edges over the low-contrast edges. Both functions consist of a free parameter k . This constant k is used to decide the validity of a region boundary based on its edge strength. To study the performance of second and fourth order PDE in removing the noise and preserving the edges, both filters were applied to the Gaussian distributed noisy image of zero mean and standard deviation of 30

and results are shown in figure 1. From the denoised image, it is inferred that both filters are performing well in removing the noise while preserving the edges for more number of iterations (50).

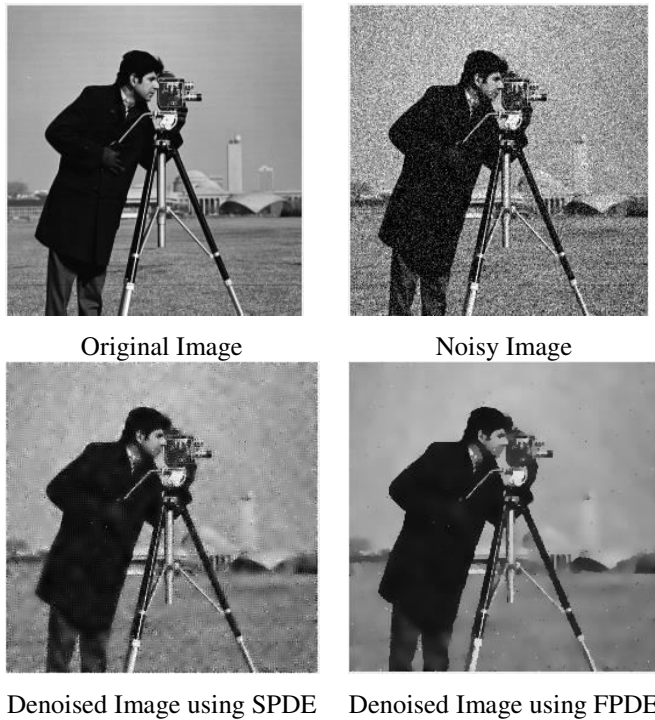


Figure 1: Noisy and Denoised Images using Second and Fourth Order Partial Differential Equations

III. PROPOSED METHODOLOGY

The proposed method to perform multi focused image fusion needs three steps as shown in the figure 2. In first step, each source image is decomposed into approximation and detail images by employing edge preserving second and fourth order PDE. In the next step, approximation and detail images are fused by employing separate fusion rules and the different fusion methods are given below. Final fused image is reconstructed by combining the final fused approximation and detail images [5].

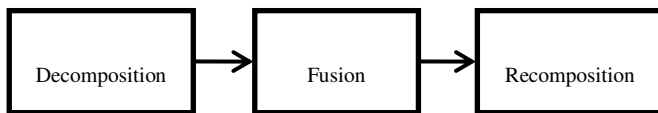


Figure 2: Method of Multi Focused Image Fusion

Let the source images be $I_n(x,y)$, where $n = 1,2$ and all source images are assumed to be registered spatially. These images are passed through edge preserving second and fourth order PDE filter to separate into approximation and detail images. Let $A_{nj}(x,y)$ be the low frequency band of source image $I_n(x,y)$ after j^{th} iteration of second and fourth order PDE filter. The high frequency band $D_{nj}(x,y)$ are obtained by subtracting $A_{nj}(x,y)$ from $I_n(x,y)$. The low frequency bands contain the average image information whereas the high frequency bands contain detail information. So, it is necessary to have different feature

selection decision mechanism to select the coefficients from the low frequency and high frequency bands as shown in Fig 3. The fast and efficient fusion rules were employed to combine low and high frequency band to select the coefficients from low and high frequency band. To fuse high frequency band images, Principal Component analysis is used whereas fusion rule ranging from average to various focus measures were used to fuse the low frequency band images.

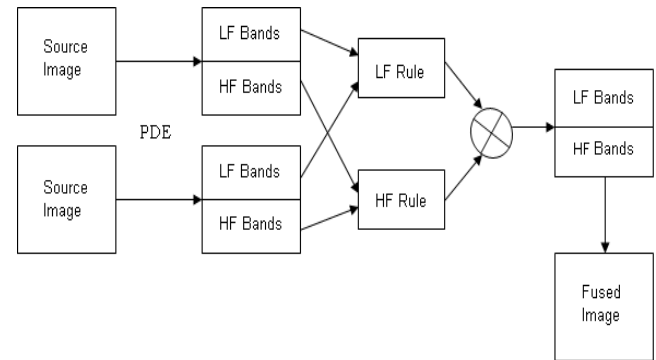


Figure 3: Proposed Multi Focused Image Fusion

Method 1: This method uses the same activity measure to select the coefficients from high and low frequency bands to form fused image. The optimal weights based on principal component analysis are used to select the required information from high and low frequency band images and to form the final fused image. To find the principal component value, each high frequency bands ($D_{1j}(x,y), D_{2j}(x,y)$) are considered as column vectors of a matrix M . The covariance matrix C_{MM} of matrix M is found by taking each row as an observation and each column as a variable. Next the Eigen values λ_1 & λ_2 and corresponding Eigen vectors Φ_1 & Φ_2 of C_{MM} are calculated. Let λ_{max} be the largest Eigen value from λ_1 & λ_2 and corresponding Eigen vector be Φ_{max} . Calculate principal components P1 and P2 corresponding to Φ_{max} by normalizing their values as follows:

$$P1 = \frac{\Phi_{max(1)}}{\sum_i \Phi_{max(i)}}, P2 = \frac{\Phi_{max(2)}}{\sum_i \Phi_{max(i)}} \dots \dots (4)$$

These principal components P1 and P2 act as weights to fuse high frequency bands into final high frequency band.

Method 2: This method uses separate activity measure for low and frequency sub bands. The objective of any image fusion algorithm is to identify, compare and transfer the important visual information from source images into a fused image without any loss. Visual information is conveyed by gradients and edges in images. Since, low and high frequency sub bands contain different information, a good image fusion algorithm should deal the low frequency and high frequency sub bands separately. This method uses Li activity measure [6] to fuse low frequency bands and principal component analysis to select the coefficients from high frequency bands.

Method 3: In this method, the salience match measure based fusion rule [7] is applied to the low frequency bands

and principal component analysis is used to select the coefficients from high frequency bands. The salience of low frequency band is computed as a local energy in the neighborhood of a coefficient. The salience of coefficient 'p' of band 'A' over an window is denoted as E(A,p) and calculated as:

$$E(A, p) = \sum_{\varphi=Q} W(q)C_j^2(A, q) \dots\dots (5)$$

where w(q) is a weight and $\sum_{\varphi=Q} w(q)=1$. At a given decomposition level j, this fusion scheme uses two distinct modes of combination namely Selection and Averaging. In order to determine whether the selection or averaging to be used, the match measure M(p) is calculated as:

$$M(p) = \frac{2 \sum_{\varphi=Q} W(q)C_j(A, q)C_j(B, q)}{E(A, p) + E(B, p)} \dots\dots (6)$$

If M(p) is smaller than a threshold T, then selection mode is used. In this mode, the coefficient with the largest local energy is placed in the composite transform. It is implemented as:

$$C_j(F, p) = \begin{cases} C_j(A, p), E(A, p) \geq E(B, p) \\ C_j(B, p), E(B, p) > E(A, p) \end{cases} \dots\dots (7)$$

If $M(p) \geq T$, then averaging mode is used to form the composite transform coefficient. It is implemented as:

$$C_j(F, p) = \begin{cases} W_{\max} C_j(A, p) + W_{\min} C_j(B, p), E(A, p) \geq E(B, p) \\ W_{\max} C_j(B, p) + W_{\min} C_j(A, p), E(B, p) > E(A, p) \end{cases} \dots\dots (8)$$

where $W_{\min} = 0.5 - 0.5 \left(\frac{1 - M(p)}{1 - T} \right)$ & $W_{\max} = (1 - W_{\min})$

A binary decision map is used to record the coefficient selection results. If the coefficient is from image 'A', the logic value '1' is stored in the map. Otherwise, logic value '0' is stored. Then, consistency verification is applied to this binary decision map. The fused coefficient map is generated based on new binary decision map. The fused image is obtained by applying inverse transform on fused coefficient map.

Method 4: In this method, absolute of maximum value as activity measure is used to fuse the low frequency band. This activity measure preserves dominant features at each scale in the fused image. The low frequency bands contain the average image information. Since larger absolute coefficients correspond to sharper brightness changes, the absolute maximum value is used as activity measure for low frequency bands.

Method 5: This method uses average value as activity measure to fuse low frequency bands and principal

component analysis to select the coefficients from high frequency bands.

IV. RESULTS AND DISCUSSIONS

Analysis and Experimental results are provided in this section to find out the strength of second and fourth order partial differential equations to arrive an efficient way to fuse multi focused images. The multi focus image fusion based on second and fourth order partial differential equations are implemented using MATLAB simulation package. These approaches are tested with 10 images and the factors considered for analysis are Quality Index (QI) [8] and feature mutual information values based on Gradient MI (Gradient) and Edges MI (Edge) [9-10]. The average value of performance metrics for all test images are shown in the following Table 1 and from the table it is inferred that Method 5 outperforms well for both second and fourth order partial differential equations. Also the tested images with its fused images using second and fourth order partial differential equations are shown in figure 3 for qualitative evaluation. From that figure, it is inferred that Method 5 outperforms other fusion methods and fused images using fourth order PDE gives clear idea of the scene without artifacts compared to other methods.

Table I : Quantitative Results of Multi Focused Image Fusion using SPDE and FPDE

Method 1	SPDE	FPDE
QI	0.80761	0.80765
MI(Gradient)	0.65487	0.65491
MI(Edge)	0.90302	0.90301
Method 2	SPDE	FPDE
QI	0.76503	0.77169
MI(Gradient)	0.61565	0.63096
MI(Edge)	0.89343	0.90335
Method 3	SPDE	FPDE
QI	0.80752	0.8076
MI(Gradient)	0.65305	0.65378
MI(Edge)	0.90201	0.90185
Method 4	SPDE	FPDE
QI	0.77447	0.77483
MI(Gradient)	0.62277	0.64075
MI(Edge)	0.89541	0.89293
Method 5	SPDE	FPDE
QI	0.80861	0.81166
MI(Gradient)	0.65488	0.65493
MI(Edge)	0.90303	0.90305



Figure 4: Results of Multi Focused Image Fusion using SPDE and FPDE

V. CONCLUSIONS

This paper compares and presents the application of second and fourth order partial differential equations in multi focused image fusion. Five methods of multi focused image fusion was implemented and tested with 10 sets of images. From the results, it is inferred that average value as activity measure to fuse low frequency bands and principal component value as activity measure to fuse high frequency bands produces best results for both second and fourth order PDE. In addition to that it, fourth order PDE outperforms second order PDE for all methods of multi focused image fusion and produces best results in terms of Quality Index, Gradient based Mutual Information and Edges based Mutual Information.

REFERENCES

- [1] Yong Yang, Yue Que, Shu-Ying Huang, Pan Lin, "Technique for multi-focus image fusion based on fuzzy-adaptive pulse-coupled neural network", *Signal, Image and Video Processing*, 11(3), 2016, 439-446
- [2] Durga Prasad Bavirisetti and Ravindra Dhuli, "Fusion of Infrared and Visible sensor images based on Anisotropic diffusion and Karhunen Loeve Transform", *IEEE Sensors Journal*, 16(1), 2015, 203-209.
- [3] Perona P, and Malik J, "Scale-space and edge detection using anisotropic diffusion," *IEEE Trans. Pattern Anal. Mach. Intell.*, 12(7), 1990, 629–639.
- [4] You Y L, and Mostafa Kaveh. "Fourth-order partial differential equations for noise removal." *IEEE Transactions on Image Processing*, 9(10), 2000, 1723-1730.
- [5] Durga Prasad Bavirisetti, Gang Xiao, Gang Liu. "Multi-sensor image fusion based on fourth order partial differential equations" , *20th International Conference on Information Fusion (Fusion)*, 2017.
- [6] S. Li and B. Yang, "Multifocus image fusion using region segmentation and spatial frequency", *Image and Vision Computing*, 26 (7), 2008, 971-979.
- [7] Xiaoye Zhang, Yong Ma, Fan Fan, Ying Zhang, and Jun Huang, "Infrared and visible image fusion via saliency analysis and local edge-preserving multi-scale decomposition," *J. Opt. Soc. Am. A*, **34**, 2017, 1400-1410.
- [8] Wang Z., Bovik A.C., Sheik H. R. and Simoncelli E. P., "Image Quality Assessment: From Error Visibility to Structural Similarity", *IEEE Trans. Image Processing*, 13, 2004.
- [9] Haghghat, M., Aghagolzadeh, A., Seyedarabi, H., "A Non-Reference Image Fusion Metric Based on Mutual Information of Image Features," *Computers and Electrical Engineering*, 37(5), 2011, 744-756.
- [10] Haghghat, M., Razian, M.A., "Fast-FMI: non-reference image fusion metric," *Proc. 8th International Conference on Application of Information and Communication Technologies (AICT)*, 2014, 1-3.
- [11] Dhirendra Pal Singh, "Role of Statistical Parameter in Digital Image Enhancement", *Int. J. Advanced Networking and Applications*, 11(4), 2020, 4350-4353.
- [12] Gan W., Wu X., Wu, W., Yang, X., Ren, C., He, X., and Liu, K., "Infrared and visible image fusion with the use of multi-scale edge-preserving decomposition and guided image filter," *Infrared Physics & Technology*, 72, 2015, 37–51.
- [13] He K., Sun J., and Tang, X. , "Guided image filtering," in *Proc. Eur. Conf. Comput. Vis., Heraklion, Greece*, 2010, 1–14.
- [14] He K., Sun J., and Tang, X. , "Guided image filtering," *TPAMI*, 35(6), 2013,1397–1409.
- [15] Li, S., Kang, X. and Hu, J., "Image fusion with guided filtering," *Image Processing, IEEE Transactions on* 22, 2013, 2864–2875.
- [16] Zhou, Z., Wang, B., Li, S. and Dong, M., "Perceptual fusion of infrared and visible images through a hybrid multi-scale decomposition with gaussian and bilateral filters," *Information Fusion*, 30, 2016, 15–26.
- [17] <http://www.image-net.org/index>
- [18] <http://www.metapix.de/toolbox.htm>